Massey University Library. Thesis Copyright Form

Title of thesis: Rotating Frame Relaxation of Polymer Melts

(1) (a) I give permission for my thesis to be made available to readers in the Massey University Library under conditions determined by the Librarian.

~~(b) I do not wish my thesis to be made available to readers without my written consent for _____ months.~~

(2) (a) I agree that my thesis, or a copy, may be sent to another institution under conditions determined by the Librarian.

~~(b) I do not wish my thesis, or a copy, to be sent to another institution without my written consent for _____ months.~~

(3) (a) I agree that my thesis may be copied for Library use.

~~(b) I do not wish my thesis to be copied for Library use for _____ months.~~

Huiras

Signed Paul Callaghan (for T.M. Huiras)

Date 16/3/89

The copyright of this thesis belongs to the author. Readers must sign their name in the space below to show that they recognise this. They are asked to add their permanent address.

NAME AND ADDRESS	DATE

Rotating Frame Relaxation in Polymer Melts

A thesis presented in partial fulfilment of
the requirements for the degree of
Master of Science
in Physics at
Massey University

by

Te Whitinga Mark Huirua

1988

Maori Proverb

Ehara ta te tangata kai, he kai titongi kau;
engari mahi ai ia ki te wherna; tino kai, tino makona.

(Food provided by someone else is only food to be nibbled;
food produced by one's own labour on the land is good, satisfying food).

" Writing a book is an adventure. To begin with, it is a toy
and an amusement. Then it becomes a mistress, then it
becomes a master, then it becomes a tyrant. The last phase
is that just as you are about to be reconciled to your servitude,
you kill the monster and fling him about to the public ".

... Sir Winston Churchill

Abstract

Entangled high polymers in the melt or semidilute solution exhibit motion dependent on the timescale. This motion may be characterised in terms of the " tube model " in which the random coil polymer under investigation is enclosed in a tube formed by its neighbours. At the shortest timescale, motion consists principally of segment reorientation. The topology of the tube implies that some residual anisotropy will exist in this motion[3]. On the next higher timescale reptative displacements around tube bends occur, thus causing a fluctuation in the direction of residual orientation. On the longest timescale, final correlation loss occurs by tube renewal.

$T_{1\rho}$ is the relaxation time for a spin system to come to thermal equilibrium in a transverse RF field. It is sensitive to components of the motion at the RF Larmor frequency. This frequency is low and adjustable (10^2 to 10^5 Hz) and extends the regime accessible to Field cycling T_1 experiments[4]. $T_{1\rho}$ therefore provides access to the intermediate and long timescale fluctuations in entangled polymers. It is a major conclusion of this work that reptation and tube renewal effects can be directly observed.

The BPP theory of relaxation[25] has been extended to $T_{1\rho}$ for three proton spins in a methyl group. Results of a relaxation study in two polymer melt systems, namely polydimethylsiloxane and polyethylene oxide are presented. In the latter case the results are compared with $T_{1\rho}$ dispersions made on Polyethylene melts[13]. The experimental data is seen to follow the theoretical predictions made by Kimmich[3,4].

Acknowledgements

I wish to express my sincere gratitude to the following people for their involvement in this work:

My supervisor Prof. Paul Callaghan for providing both theoretical and technical knowledge when most needed as well as an " extra hand " at experiment (" harvest ") time. His great insight and unlimited enthusiasm for Physics gave encouragement enabling me to complete this task.

Dr Craig Eccles for his interest and assistance in the probe development.

The Mechanical Workshop Staff for the construction of the probe body.

The Electronic Workshop Staff for their practical suggestions and tips throughout the development of the hardware.

Fellow post-graduate students Yang Xia, Peter Daivis, Peter Saunders, James Conway, and Andrew Coy for both their educated and uneducated opinions and discussions throughout the course of this work. " Pawn to King four !! ".

Dr Rosie Wang who shared in the long hours necessary, at " harvest " time, to gather experimental data. Your empathy is greatly appreciated.

Dr Ted Garver whose keen interest was shown to me through constructive comments, good questions, and all round support during the writing of this thesis.

The Education Department for providing financial support through the award of a Maori and Polynesian Scholarship for Higher Education.

The Department of Scientific and Industrial Research for providing financial support through the award of a Post-graduate Scholarship.

The Maori Education Foundation, the Taranaki Trust Board, and the Wanganui Trust Board for providing financial assistance enabling me to continue.

Massey University for providing financial assistance and the opportunity to carry out this research.

And of course To'aiga Su'a, my fiancee at the present time of writing, whose unfailing love and support provides an all-win situation in everything I do.

Contents

Title page i
Maori Proverb ii
Quotation iii
Abstract iv
Acknowledgements v
Contents **vi**
List of Figures viii
Tables and Photographic Plates x
List of Symbols xi

Chapter 1 Introduction **1**
1.1 Polymer Melt Dynamics 1
1.2 The Relationship Between NMR Relaxation Times and the Spectral Densities 3
1.3 The " Tight Tube " Condition and the Polymer Melts
1.4 T_1 Dispersions - The Experiments of Kimmich et al 4

Chapter 2 Basic NMR Theory **5**
2.1 Historical 5
2.2 NMR Theory 6
2.2.1 Nuclear Magnetism
2.2.2 Precession 7
2.2.3 The Density Matrix 9
2.2.4 The Bloch Equations and Relaxation Times 10
2.2.5 The Density Matrix Description of State Populations 13
2.3 NMR Observables 14
2.4 Description of NMR Pulse Sequences 14
2.4.1 Single 90° Pulse 14
2.4.2 Spin-locking 15
2.4.3 Spin-echoes 17

Chapter 3 Theory of Relaxation **19**
3.1 Introduction 19
3.1.1 The Assumption of a Spin Temperature 19
3.1.2 Consideration of the Reservoir from an Energy Viewpoint 20
3.1.3 Derivation of Hebel-Slichter Expression for T_1 21
3.2 Derivation of the Spin-lattice Relaxation Times 23
3.2.1 Relaxation along the Static Field 23
3.2.2 Relaxation along the Rotating Field 29
3.3 The Problem of the Rotating Methyl Group 30
3.3.1 General 30
3.3.2 Rapid Rotation 34

Chapter 4 Derivation of the Spectral Densities **36**
4.1 Rotational Diffusion Outlined 36
4.1.1 Autocorrelation of $F_k(t)$ with Spherical Freedom 36
4.1.2 Autocorrelation of $F_k(t)$ with Azimuthal Freedom only 37
4.2 Application to the Methyl Group 38
4.2.1 First Steps 38
4.2.2 Identification of the ϕ_k and the Derivation of $J_0(\omega)$ 39

4.3 T_1 and $T_{1\rho}$ for Rapid Rotation 41
4.4 Polymer Motion 42
4.4.1 The Kimmich Model 42
4.4.2 Component A: Local Processes 43
4.4.3 Component B: Semi-Local Processes 43
4.4.4 Component C: Global Processes 45
4.5 Summary of the Spectral Density 46

Chapter 5 Hardware and Software 48
5A Hardware 48
5A.1 General Outline of the $T_{1\rho}$ System 48
5A.2 RF Probe 49
5A.2.1 RF Coil 49
5A.2.2 High Voltage Capacitors 51
5A.2.3 Series-Parallel Tank Circuit 51
5A.2.4 Electrical Current Shims 56
5A.2.5 Coil Holder 58
5A.3 Duplexor 60
5A.4 Henry Radio 1kW Linear Amplifier and Driver 62
5A.4.1 Exciter / Preamplifier 62
5A.4.2 Henry Radio 1kW Linear Amplifier - Model 2006 66
5A.5 60MHz Receiver 68
5A.6 TI-980A Computer 68
5B Software 69
5B.1 Software Outline 69
5B.2 Set Parameters 75
5B.2.1 Hex Monitor 75
5B.2.2 ' T ' - Times 77
5B.2.3 ' L ' - Level 78
5B.2.4 ' R ' - Run Processing 78
5B.3 Running the Experiment 79
5B.4 Memory Organisation 81

Chapter 6 Data Analysis 82
6.1 Modelling the Observed Behaviour 82
6.2 The Coupled Two-spin System 85
6.3 Experimental Results 87
6.4 Comparison with Theory (Discussion and Interpretation) 92
6.4.1 PEO(PEG) Data 92
6.4.2 PDMS Data 97

Chapter 7 Conclusion 102

Appendix A Spin 1 analysis of Spin-echo 104

Appendix B Derivation of the Spectral Densities J_1 and J_2 106

Appendix C Spectral Density Function of Kimmich 109

Appendix D J component of $T_{1\rho}$ for Isotropic Rotational Diffusion 112

Appendix E Program Listing 113

Bibliography 127

List of Figures

Fig.1-1	A chain in polymer melts confined to a tight tube	2
Fig.1-2	Log J_0 (ω) dispersion predicted by the reptation model of Kimmich	3
Fig.2-1	Energy level separation in a spin 1/2 system	6
Fig.2-2	Rotation of $M_z = M_0$ into the x-y plane in a time t_{90}	9
Fig.2-3	Exponential decays of M_x and M_y with time constant T_2	11
Fig.2-4	Exponential decay of M_z with time constant T_1	12
Fig.2-5	Phase coherence and phase incoherence of a two-spin system	13
Fig.2-6	90° RF pulse sequence	15
Fig.2-7	M_0 relaxing along the rotating field	16
Fig.2-8	Spin-locking RF pulse sequence	15
Fig.2-9	The Carr-Purcell spin-echo	18
Fig.3-1	Energy coupling between the spin system and the reservoir	20
Fig.3-2	Energy exchange in a spin 1/2 system	20
Fig.3-3	The geometry for two spins i and j subject to a main magnetic field B_0	23
Fig.3-4	The geometry for the CH_3 methyl group subject to a main magnetic field B_0	31
Fig.3-5	The new axis system for the CH_3 methyl group	32
Fig.3-6	The geometry for the CH_3 methyl group shown in the y-z plane	32
Fig.3-7	The geometry for the CH_3 methyl group shown in the plane normal to z	33
Fig.4-1	A chain in polymer melts confined to a tight tube	42
Fig.4-2	Segmental reorientation	43
Fig.4-3	Curvilinear diffusion	44
Fig.4-4	Log J_0 (ω) dispersion predicted by the reptation model of Kimmich	47
Fig.5-1	Block diagram of the FX60 spectrometer	48
Fig.5-2	The RF coil	50
Fig.5-3a	The high voltage capacitor	52
Fig.5-3b	The mounting of the two high voltage capacitors (**Photograph**)	**53**
Fig.5-4	Parallel-series RF tank circuit	54
Fig.5-5	Split-capacitor RF tank circuit	55
Fig.5-6	The RF tuning circuit	56
Fig.5-7	The Z gradient shim coil	57
Fig.5-8	The Y gradient shim coil	58
Fig.5-9a	The X,Y, and Z gradient shim coils (**Photograph**)	**59**
Fig.5-9b	The location of the shim coils on the RF probe (**Photograph**)	**59**
Fig.5-10	A single duplexor	60
Fig.5-11	The practical duplexor set-up	60
Fig.5-12	Duplexors in parallel; capable of withstanding high voltages (**Photograph**)	**61**
Fig.5-13a	Henry radio amplifier (above) with Driver unit (**Photograph**)	**63**
Fig.5-13b	Exciter / preamplifier circuit diagram	64
Fig.5-14a	Exciter / preamplifier Power Out vs. Power In	65
Fig.5-14b	Exciter / preamplifier Gain vs. Power In	65
Fig.5-15	Henry radio amplifier circuit diagram	66
Fig.5-16	Henry radio amplifier Power Out vs. Power In	67
Fig.5-17	Block diagram of the 60MHz receiver	68
Fig.5-18a	Flowchart for a T1RHO Experiment	70

Fig.5-18b	Flowchart for Data Analysis	71
Fig.5-18c	Flowchart for selection of " Times "	72
Fig.5-18d	Flowchart for selection of " Level "	73
Fig.5-18e	Flowchart for selection of " Run processing "	74
Fig.5-19	T1RHO menu	69
Fig.5-20	The four modes of operation: ' R ', ' L ', ' T ', ' M '	75
Fig.5-21	Hex. monitor	76
Fig.5-22	Time mode selected	77
Fig.5-23	RF Level selection	78
Fig.5-24	Accumulation menu	79
Fig.5-25	Template pulse sequence	80
Fig.6-1	PEO(PEG) and PE plots at 555Hz showing bi-exponential decay	84
Fig.6-2	The coupled two-spin system	86
Fig.6-3	PEO(PEG) raw data	90
Fig.6-4	PEO(PEG) ' coupled two-spin ' data	90
Fig.6-5	PDMS data at room temperature RT = 26°C	91
Fig.6-6	PDMS data at high temperature of 150°C	91
Fig.6-7	PEO(PEG) data with theoretical fit	93
Fig.6-8	PE data reproduced from reference (13)	94
Fig.6-9	" Stored lengths " in a chain	98
Fig.6-10	PDMS data (26°C) with theoretical fit	99
Fig.6-11	PDMS data (150°C) with theoretical fit	100
Fig.6-12	Interdependence of a_2 and τ_1 for PE fit	101
Fig.A-1	Spin-echo pulse sequence	104
Fig.C-1	Cos $\phi_{i,j}$ and Sin $\phi_{i,j}$ relationships in Kimmich spectral densities	109

Tables and Photographic Plates

Table 5-I	RF coil measurements at 60MHz	51
Table 6-I	The data from the two-spin coupled bath model	88,89
Table 6-II	Correlation times and anisotropy constants for the two polymer melt systems	95
Fig.5-3b	The mounting of the two high voltage capacitors	53
Fig.5-9a	The X,Y, and Z gradient shim coils	59
Fig.5-9b	The location of the shim coils on the side of the RF probe	59
Fig.5-12	Diodes in parallel; capable of withstanding high voltages	61
Fig.5-13a	Henry Radio amplifier (above) and Driver unit	63

List of Symbols

Symbol

a	Anisotropy constant
a	Radius of sphere
a_{mj}	Complex admixture amplitudes
$\mathbf{B}_0$	Main magnetic field directed along the z axis
$\mathbf{B}_1$	Applied RF field
c	The Curie constant
c.c	Complex conjugate
C	Capacitance
d	Diameter of wire
D	Diffusion coefficient
E	Energy
f_0	Larmor frequency
f_1	Frequency of applied field
$F_i(t)$	Spatial operator where i = 0,1,2
$\mathbf{F}$	Fourier transform operator
G	Correlation function
$\hbar$	Plancks constant divided by 2π
$\mathcal{H}$	Energy Hamiltonian
i	$(-1)^{1/2}$
I	Electrical current
I	Nuclear spin quantum number
j	Total angular momentum quantum number
$J_i(\omega)$	Spectral density for a two spin system where i = 0,1,2
J	Spin magnetisation
k	Boltzmanns' constant
$K_{ij}(\omega)$	Spectral density for an N spin system
l	Length of the RF coil
l	Mean path length
L	Inductance
L_0	Extended tube length
m	Azimuthal or magnetic quantum number
M_c	Critical entanglement molar mass
M_N	Number average molar mass
M_W	Weight average molar mass
$\mathbf{M}$	Macroscopic magnetisation vector
n	Number of turns on the RF coil
N	Number of spins per unit volume
$p_{\pm 1/2}$	Relative probability of finding a spin in the state $m_j = \pm 1/2$
p_n	Population of the nth energy level
$P(\Omega, \Omega_0, t)$	Conditional probability of finding the system at Ω at time t if it is at Ω_0 at time zero
Q	Quality factor of RF coil
r	Diameter of RF coil
r	Internuclear separation
r	Radius of coaxial cylinder

r'	Matching impedance
R	Resistance
s	Scaling factor
S	Resultant NMR signal
t	Time parameter
t_{90}	$\pi / 2$ pulse time
T	General temperature
T_L	Lattice temperature
T_s	Spin temperature
T_1	Spin-lattice relaxation time
T_2	Spin-spin relaxation time
$T_{1\rho}$	Rotating frame spin-lattice relaxation time
Tr	Trace of a matrix
$U_E(t)$	Evolution operator
$U_{RZ}(\theta)$	Rotation operator
W_{nm}	Transition probability between quantum levels $\|n>$ and $\|m>$
x	Distance parameter
Y_n	Spherical harmonic of order n
$2Z_0$	Width of RF probe (Spacing between the shim coils)

α	Angle between main magnetic field and the methyl group
β	Rotation about the methyl bond
$\hat{\beta}$	Equal to $1 / kT$
γ	Gyromagnetic ratio
γ	Rotation of the methyl group about the magnetic field
δ	Skin depth
Δ_s	Laplacian operator on the surface of a sphere
Δ_0	Mean tube length per fold
ε	Dielectric constant
ε_0	Permittivity of free space
η	Parameter of shim coil
θ	Polar angle
λ	Wavelength
μ_z	z magnetisation
μ_0	Permeability of free space
ρ	Resistivity
ρ	Density matrix
σ	Proximity factor
τ	Correlation time
ϕ	Azimuthal angle
$\Psi(\theta,\phi)$	Probability of finding the internuclear vector at (θ,ϕ) at time t
ω_0	Larmor precession frequency due to B_0
ω_1	Larmor precession frequency due to B_1

$< A >$	Observable
$\mid jm_j >$	Basis set of eigenstates
$\mid \Psi >$	General state of a nuclei
*	Complex conjugate

Chapter 1 Introduction

Pawn to King four

1.1 Polymer Melt Dynamics

Molecular motion in polymer melts can be studied using NMR relaxation time measurements to probe the spectral densities which are based on fluctuating dipolar interactions between nuclear spins.

It has been shown[1] that there are two types of viscoelastic behaviour. Low molecular mass polymers behave similar to isolated polymers and follow the predictions made by Rouse[2]. The high molecular mass spectrum, however, can be separated into a high frequency component and a low frequency component. The high frequency component is similar to that observed in the low molecular mass polymers. The low frequency component exists due to the effects of entanglements in polymer melts. The molecular mass at which the characteristics of the melt change is designated the critical molecular mass, M_c . It is the topic of this thesis to study the behaviour of polymer chains of masses higher than M_c, since this is the regime where entanglements occur, and it is the effect of these entanglements which govern the overall motion.

The motion can be separated into three components[3]. In the shortest timescale, that of the "local" (and therefore molecular weight independent processes) the motion is largely due to segment re-orientation by diffusing local " defects " (rotational isomers of neighbouring segments). This motion can be considered to correspond to the diffusion of a particle between two reflecting barriers[4,5] with correlation time τ_s.

Since the polymer chains are not able to pass through each other they are effectively confined inside a tight-tube region (see Fig.1-1).This tube which surrounds the chain is not fixed in space but is constantly renewed as the chain diffuses throughout the tube[6]. This curvilinear chain diffusion, known as a a " semi-local " process, occurs in the intermediate timescale with correlation time τ_l . The dynamics of such a process has been studied by de Gennes[7] who shows that local defect diffusion is the elementary process which finally causes the " reptation " phenomenon; the motion is due to further segment re-orientation by reptative displacements around bends of the tight-tube.

The centre line of the tube, called the primitive chain by Doi & Edwards[6], moves randomly forwards or backwards only along itself. The chain ends are free, therefore, to orient themselves randomly. It is the reptative process which finally leads to the transportation of material to and from the chain ends causing the surrounding tube to thread itself into a new configuration. This tube renewal, a " global " process, occurs in the largest timescale with correlation time τ_r .

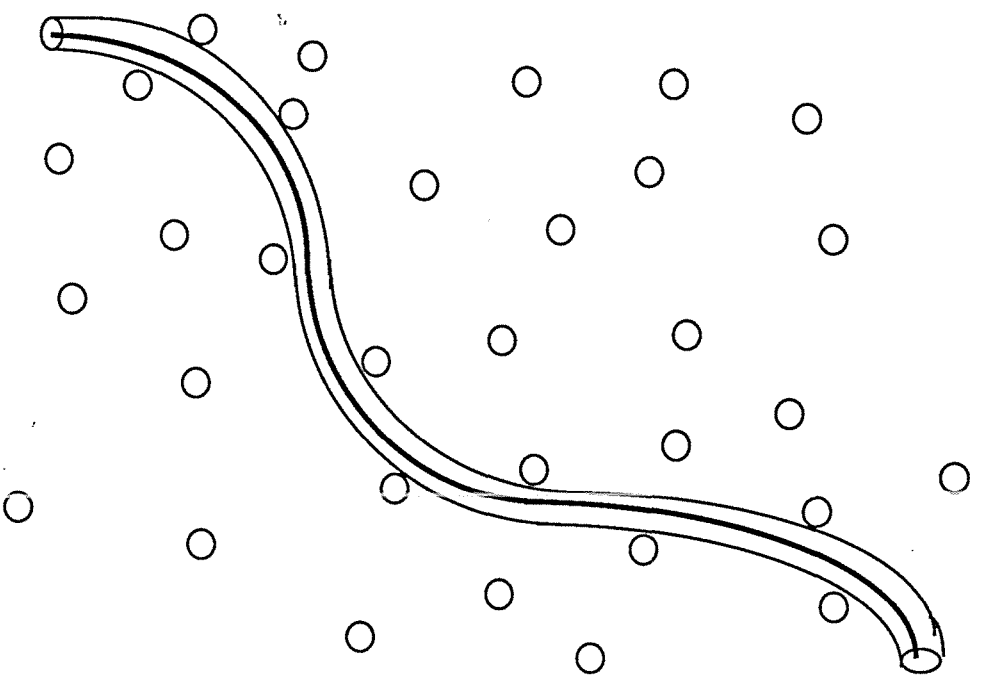

Fig.1-1

Schematic illustration of a chain in polymer melts. The chain is confined to a tight tube formed by the matrix of neighbouring chains (circles).

1.2 The Relationship Between NMR Relaxation Times and the Spectral Densities

The relaxation phenomenon is caused by the fluctuating dipolar interactions arising from the tumbling of the molecule. Although this tumbling motion is a random process it can be characterised by a correlation time, τ_c. By taking the Fourier transform of the correlation functions the spectral densities can be obtained. If the conditions of BPP[8] apply then by measuring T_1, the spin-lattice relaxation time, and T_2, the spin-spin relaxation time, information can be gained relating to the spectral densities at the characteristic frequencies of zero, ω_0 and $2\omega_0$ where ω_0 is the Larmor precession frequency about the main field B_0.

When $T_{1\rho}$ is measured, the spin-lattice relaxation time in the rotating frame, it is possible to probe the low frequency regime, while maintaining the high field sensitivity, and extract information at the characteristic frequency $2\omega_1$, where ω_1 is the Larmor precession frequency about the RF field; hence, because ω_1 is variable, and much less than ω_0, this allows us to study slow semi-local and global processes, i.e motion sensitive to τ_l and τ_r (see Fig.1-2).

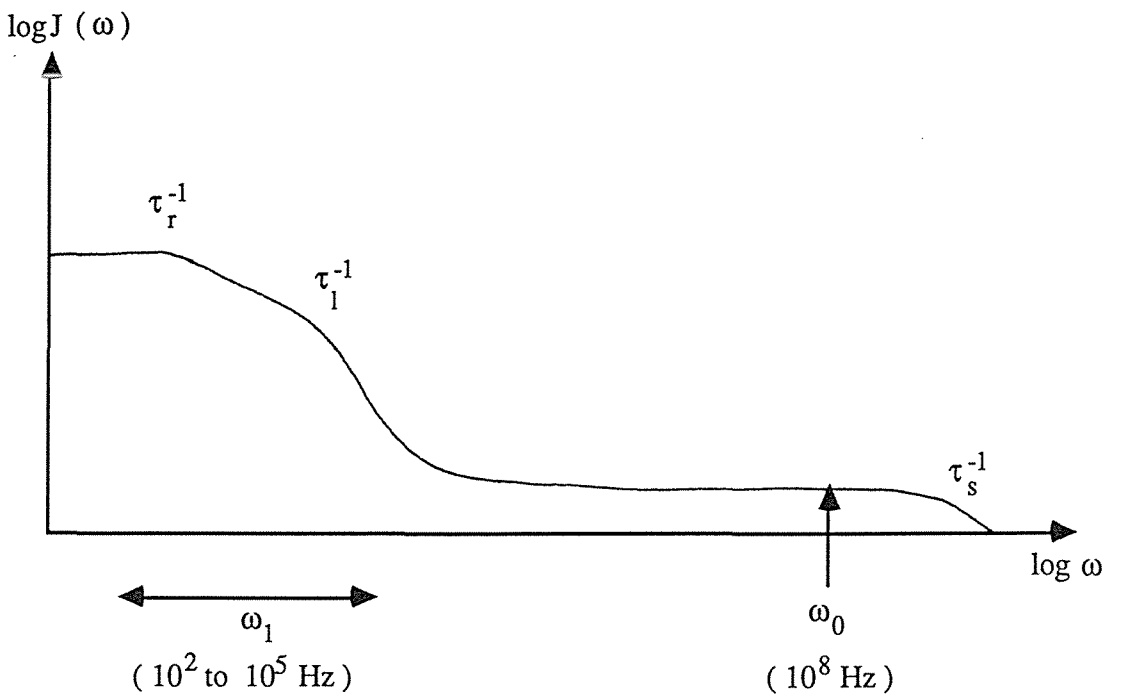

Fig.1-2

Schematic log J_0 (ω) dispersion predicted by the reptation model of Kimmich.

1.3 The " Tight Tube " Condition and the Polymer Melts

The motion of the internuclear vector causes the dipolar interaction to fluctuate. In a polymer there is a hierarchy of motion with the local segmental reorientation being most rapid and the overall molecular reorientation and centre of mass motion the slowest. If the most rapid motion involves a total correlation loss then the slow motion cannot be observed in the dipole relaxation process. The " tight tube " condition arises when the rapid processes leaves a residual correlation which remains to be modulated by slow motion. Such a residual correlation is akin to a fast local motion residual anisotropy and is characteristic of polymers in the melt. By contrast, in the solution phase the local motion is isotropic and no long range processes can be observed.

1.4 T_1 Dispersions - The Experiments of Kimmich et al

In a series of papers Kimmich and co-workers[3,4,9 - 12] have examined the dependence of the NMR longitudinal relaxation time T_1 on polarising field strengths, a technique known as field-cycling spectroscopy. Their experiments yield spectral densities at 10^4 to 10^8 Hz. In this thesis we extend this frequency range down to 10^2 Hz using $T_{1\rho}$ measurements. Two polymer systems are employed, namely, polydimethylsiloxane and polyethylene oxide. In the latter case the results are compared with $T_{1\rho}$ dispersions made on polyethylene melts[13].

It is a major conclusion of this work that $T_{1\rho}$ measurements (unlike T_1 dispersions) probe a sufficiently low frequency regime that reptation and tube renewal effects can be directly observed.